Arch. Metall. Mater. **63** (2018), 1, 473-480

DOI: 10.24425/118964

D.Y. PARK*, B.R. PARK**, C.W. GAL**, D. LIN**, J.S. HAN**, M.-S. JEONG***,
R. BOLLINA****, W. HWANG**, S.J. PARK**#

DEVELOPMENT OF HYDROPHOBIC SURGICAL FORCEPS USING POWDER INJECTION MOLDING AND SURFACE TREATMENT

Hydrophobic surgical forceps of end-effectors for laparoscopic operations or minimally invasive surgery were developed through powder injection molding (PIM) and surface treatment. Processing conditions for mixing, debinding, and sintering were investigated to produce defect-free components. An optimum solid loading was determined by torque rheometry experiments. The optimized processing conditions for debinding and sintering were designed through the measurement of weight loss and shrinkage behavior by thermogravimetric analysis and dilatometry experiments. After producing the surgical forceps based on the optimized processing conditions via PIM, surface treatment was carried out to generate the hydrophobic structure on the surface.

Keywords: Powder injection molding, hydrophobic, debinding, sintering, surface treatment

1. Introduction

The pattern on the surface of surgical forceps is conventionally fabricated by pattern rolling or cutting processes. Although the pattern rolling process offers high repeatability with close tolerances, this process could be inconvenient for producing small patterns with a high aspect ratio [1]. The cutting process involves a long production time and hence has a poor productivity rate. In order to increase productivity by reducing process time as well as increasing performance, an alternative manufacturing technology is required. In this regard, powder injection molding (PIM) that combines conventional powder metallurgy and plastic injection molding is a promising manufacturing technique to reduce production cost and produce complex shapes of components in quantity [2-3].

Stainless steel is widely used for fabricating medical devices because of its favorable mechanical properties such as high strength and reasonable corrosion resistance. Among the various types of stainless steel, 17-4PH stainless steel is an appropriate material for medical devices. Compared to the generally used stainless steel types such as the 316L and 400 series, it provides reasonable balance between corrosion resistance and mechanical strength. In this regard, 17-4PH stainless steel is generally employed for dental, medical, and surgical applications.

The determination of optimum conditions for the PIM process, consisting of four steps, is critical for producing defect-free components. The appropriate mixing and injection molding conditions determine the success or failure of subsequent PIM processes because rheological properties such as flow behavior during molding are affected by the characteristics of feedstock [4-6]. The determination of proper processing conditions for debinding processes is important to maintain the shape without the formation of defects because defects such as distortions or cracks occur most frequently in the debinding step [7-13]. Sintering, which affects dimensional tolerance as well as mechanical properties of final products, is a crucial step in the PIM process because density is a key factor that determines the quality of sintered part [14]. In this regard, it is necessary to examine densification behavior during sintering to manage the dimensional tolerance and mechanical strength of the final product parts. Hydrophobicity or water repellency is a phenomenon resulting from the relation between the surface energy of material and the surface tension of water, and has been widely utilized in many areas such as adhesion/culturing, micro-fluidics, self-cleaning, anti-fog, anti-icing, and anti-corrosion [15-21]. Although hydrophobic surfaces have been fabricated through various manufacturing techniques such as photolithography, the sol-gel method, thermal evaporation, UV illumination, electro spinning, and plasma fluorination, they are inadequate for mass production [22-23]. Therefore, a simple and inexpensive manufacturing method is required. In a similar manner, materials employed to fabricate hydrophobic surfaces are selected by the criterion of simple access for industrial application, and the simple dipping process is employed for fabrication.

* D.Y. PARK IS KOREA INSTITUTE OF ENERGY RESEARCH, SOLAR THERMAL CONVERGENCE LABORATORY, DAEGEON, S. KOREA
** POHANG UNIVERSITY OF SCIENCE AND TECHNOLOGY, DEPARTMENT OF MECHANICAL ENGINEERING, S. KOREA
*** KOREA INSTITUTE OF INDUSTRIAL TECHNOLOGY ULTIMATE MANUFACTURING TECHNOLOGY R&BD GROUP, S. KOREA
**** SCHOOL OF ENGINEERING SCIENCES, MAHINDRA ECOLE CENTRALE, INDIA

Corresponding author: sjpark87@postech.ac.kr

Laparoscopic surgery as a minimally invasive surgery is a modern surgical technique having several advantages such as reduced pain and short recovery time because of small incisions. Although there are numerous advantages for a patient, this surgery is complicated from the perspective of a surgeon. Because the surgical field of vision available through a laparoscope is limited, it is important to secure a clear view of the surgical field. During laparoscopic surgery, forceps could be stained with blood because of surface tension. The bloodstains on the pattern of the forceps can block the view of the surgeon. Therefore, unbloodied forceps may be suitable to secure a clear view of the narrow surgical field. Although blood – 55% of which comprises plasma, which is composed of approximately 92% water, 45% red cells, 1% white cells, and platelets – is different from water; water accounts for a substantial part of blood. In this regard, hydrophobic forceps were developed to lay the foundation for unbloodied forceps.

2. Experimental procedures

The water-atomized powder of 17-4PH stainless steel was provided by Epson Atmix Co. (Aomoriken, Japan). The particle sizes of D_{10}, D_{50}, and D_{90} are 3.22, 8.30, and 19.47 mm, respectively. The powder was mixed with a wax-polymer binder system composed of 57% wax (Dussek Campbell), 25% polypropylene (PP, PolyVISIONS), 15% polyethylene (PE, DuPont), and 3% stearic acid (SA, Fischer Scientific).

The critical solid loading (vol%) expressed as the ratio of powder and binder was determined by torque rheometry (Haake PolyLab QC, MCIK). The mixing speed and temperature were selected as 150 rpm and 150°C, respectively. The critical solid loading was determined at the point of rapid rise in torque and emergence of erratic values. The optimum solid loading was fixed to be 2% lower than the critical solid loading [2]. After determining the optimum solid loading, mixing was performed by a twin extruder mixer (CetaTech Inc.). The homogeneity of the powder mixture in the feedstock was evaluated by a parallel disk type of rheometer (MCR 101, Anton Paar). The viscosity of feedstock and the total mixing time were measured.

The mold for the forceps was designed and produced. It is necessary to consider the dimensional variation induced by densification during sintering to satisfy the tolerance of the final product. Injection molding was carried out with injection molding machine (TR30EH, Sodick Plustech). The processing conditions for injection molding are summarized in Table 1.

A majority of the defects such as distortion and cracking were caused by inappropriate processing conditions including those affected by thermal history and atmosphere. The injection-molded components were debound at 60ºC in *n*-hexane to remove binder components of low molecular weight including wax and SA. The immersion time for solvent debinding was determined by measuring the weight loss (wt%) with time. Thermal gravimetric analysis (TGA) was conducted by thermal gravimetric analyzer (TGA/DSC 1, Mettler Toledo) to determine the appropriate processing conditions for thermal debinding. Based on the TGA results, decomposition behavior was analyzed, and the debinding cycle was determined.

TABLE 1

Processing conditions for injection molding

Parameters			
Temperature profile			
Nozzle (°C)	150	Nozzle diameter (mm)	2.5
Barrel zone 1(°C)	150	Plunger diameter (mm)	16
Barrel zone 2(°C)	155	Back pressure (MPa)	10
Barrel zone 3(°C)	160	Cooling time (s)	20
Injection profile			
	Step 1	Step 2	Step 3
Speed (mm/s)	20	15	10
Pressure (MPa)	50	45	30

Sintering was conducted in H_2 atmosphere to prevent degradation of corrosion resistance induced by contamination with carbon, nitrogen, or oxygen. The densification behavior on sintering was examined by a dilatometry experiment (DIL402C, Netzsch). The *in-situ* shrinkage and relative density was considered to design the mold as well as estimate the mechanical strength. The thermal cycle for a dilatometry experiment is as follows: i) ramping up from 30 to 1350°C at 10°C/min; ii) holding for 1 h; and iii) cooling from 1350 to 30°C at 10°C/min. The *in-situ* sintered relative density during sintering was calculated employing Eq. (1):

$$\rho = \rho_0 \left(\frac{1}{1 - dL / dL_0} \right)^3$$

where ρ is the relative density, ρ_0 is the initial relative density, and dL/dL_0 is the engineering strain obtained from dilatometry experiment.

Surface treatments comprising microstructure fabrication and hydrophobic material coating were carried out. The microstructure is affected by various processing conditions including the chemical solution, etching time, and temperature. Chemical etching was conducted for 6 h at room temperature. Removal of the passivation layer forms a rough surface. The hydrophobic surface can be produced by coating a hydrophobic material on the component. Dried metal specimens were dipped into heptadecafluoro tetrahydrodecyl trichlorosilane solution (HDFS, Gelest, Inc.) with normal hexane (*n*-hexane, SAMCHUN Chemical) for 3 h. The volumetric ratio of HDFS and *n*-hexane was 1:1000. The HDFS is critical for maintaining a low surface energy to result in hydrophobicity and for reaction of silane with the metal surface. The coated surface was rinsed using *n*-hexane and then dried at room temperature.

3. Results and discussions

The torque rheometer experiments to determine the critical volumetric solid loading (vol%) exhibit the mixing behavior of feedstock. The torque was measured by adding 1% of solid

loading in each step at temperature of 150°C and mixing speed of 150 rpm. The torque of feedstock increased with solid loading and fluctuated until the powder and binder were uniformly distributed as illustrated in Fig. 1a. The homogeneity of mixture can be evaluated by the steady-state value of torque. The rapid rise in torque and emergence of an erratic value are regarded as indicative features of critical solid loading [2]. However, the result was ambiguous and not adequate for a decision on critical solid loading because it did not exhibit the obvious feature of solid loading as illustrated in Fig. 1a. As an alternative method, the average value and error bar were considered to determine critical solid loading as illustrated in Fig. 1b [24-25]. Although a sharp increase in torque was not observed from the slope of the curve, the error bar was dramatically increased at solid loading of 61 vol%. Therefore, the critical solid loading was determined to be 61 vol%. The solid loading for injection molding was determined as 59 vol%, which is approximately 2 vol% lower than the critical solid loading; this is because a slight excess of binder over the critical solid loading provides lubricity essential for injection molding.

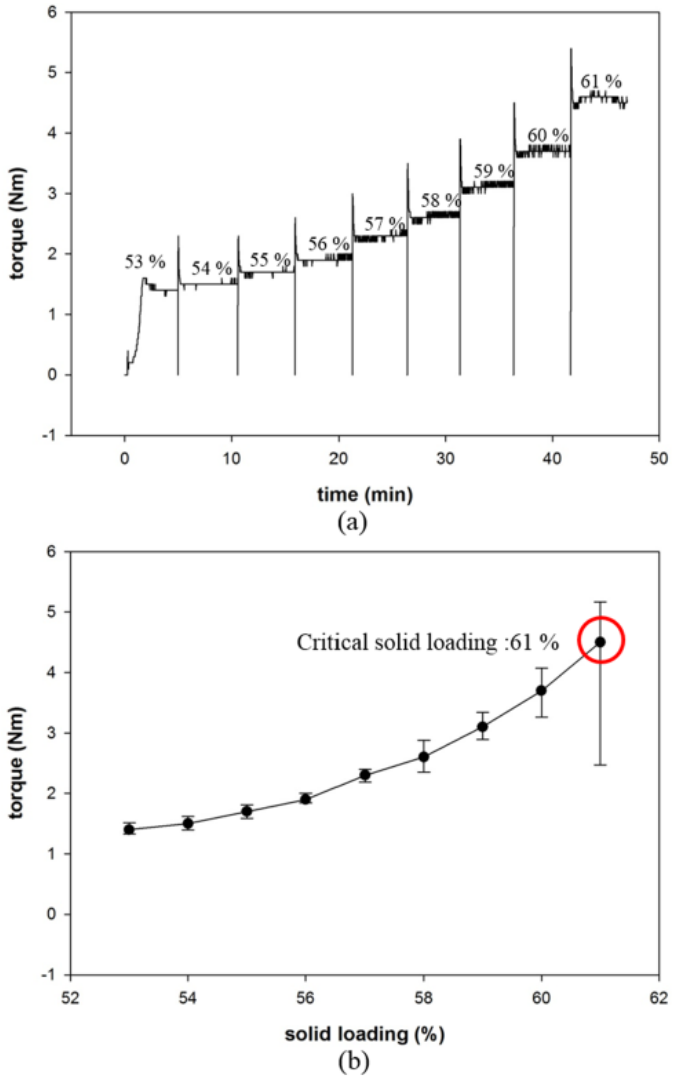

Fig. 1. Mixing behavior with different volumetric solid loading; (a) mixing torque as a function of number of times mixed at various solid loading and (b) mixing torque at different solid loading

Based on result of the torque rheometry experiment, powder and binder were mixed by the twin-screw extruder to produce the feedstock. Mixing was carried out over three times to ensure uniformity of powder and binder distribution. The feedstock homogeneity was evaluated by the viscosity variation at a constant shear rate of 100 rad/s with the number of times mixed as illustrated in Fig. 2. In the process of repeated mixing, the feedstock stabilized at a low level of viscosity. The results indicate that an increase in the number of times mixed led to the uniform distribution of powder in the binder system.

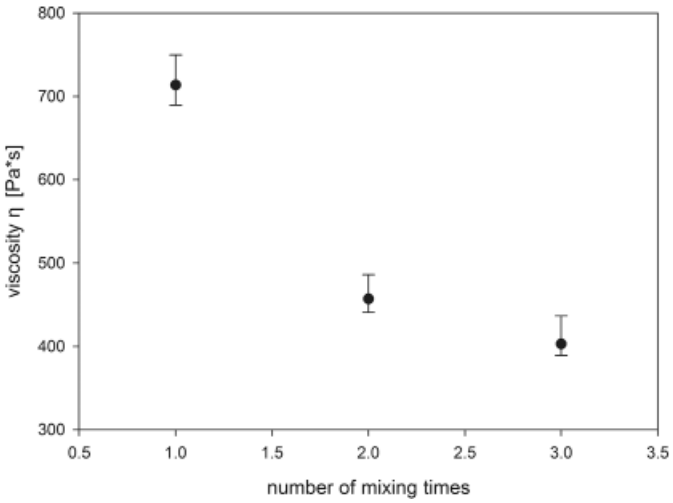

Fig. 2. Mixture homogeneity of feedstock

The surgical forceps for laparoscopic operation or minimally invasive surgery were designed as illustrated in Fig. 3a. The mold for injection molding, with consideration of shrinkage during sintering, was designed and produced. The shrinkage related to the final dimensions is presented in the results of sintering. The relatively small and complicated components including the jam member (JM), side holder (SH), and hinge pin (HP) were produced by injection molding as illustrated in Fig. 3b. The remaining components, including the forceps holder (FH), and shaft (S), were produced by machining.

A wax-polymer binder system composed of polypropylene (PP), polyethylene (PE), wax, and stearic acid (SA) was employed. The injection-molded components were immersed in *n*-hexane to dissolve binder components with relatively low molecular weight, including wax and SA. In order to determine the optimum immersion time, weight loss (wt%) was measured every two hours. The weight variation with time is presented in Fig. 4. A major portion of the binder was removed after the first two hours. Considering that the low molecular binder components including wax and SA comprised 4.42 wt% of the injection molded part, the wax and SA were fully extracted in *n*-hexane. Based on the result, the immersion time for solvent debinding was set to 2 h.

The remaining binders, including PP and PE, after solvent debinding, were removed by thermal debinding. The rate of degradation is related to the thermal properties of binders such as melting and decomposition temperatures. TGA is a measurement

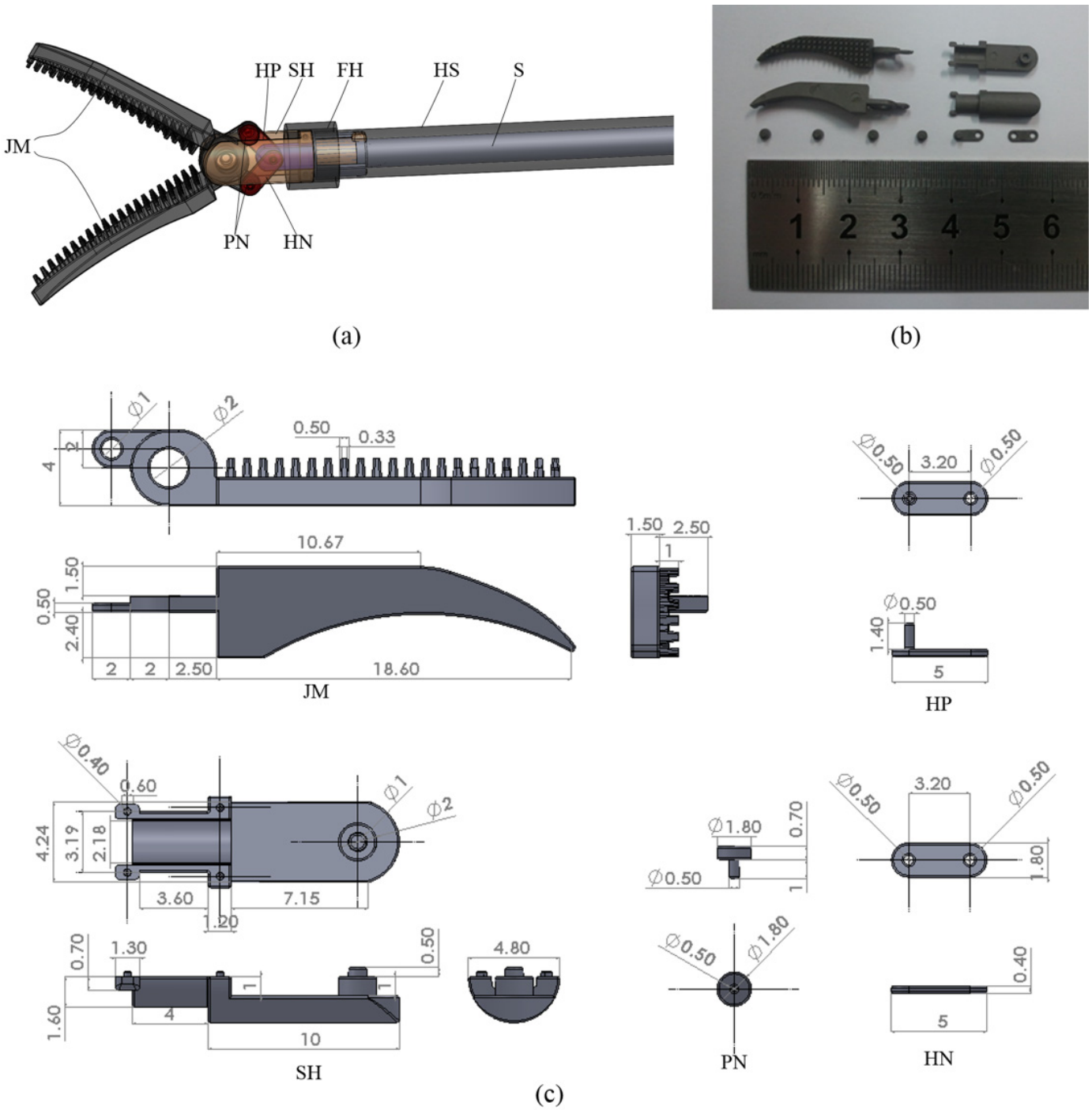

Fig. 3. Design of micro-forceps for laparoscopic operation, (a) cross-sectional CAD image JM: jaw members, SH: side holder, FH: forceps holder, HP: hinge pin, HS: hollow shaft, S: shaft, PN: pin, HN: hinge, (b) injection molded components, (c) dimensions of each component

method of weight change under a specified thermal condition. This experiment provides quantitative information on decomposition behavior to analyze weight loss and optimize processing conditions. Fig. 5a,b present the results of TGA experiments for individual binder components and feedstock at heating rate of 5°C/min in H_2 atmosphere. The ranges of decomposition temperature for PP, PE, SA, and wax were calculated by onset values as 276.80-452.86, 424.94-496.07, 190.47-283.50, and 184.50-311.54°C, respectively. A minimum temperature of 496.07°C was required to remove all binders in the injection molded part because PE having the highest decomposition temperature was fully decomposed at 496.07°C. It can also be observed that individual decomposition behaviors of binder components were in close agreement with the experimental result of feedstock. As illustrated in Fig. 5b, the residual weight of feedstock was 92.49 wt%. This result indicated that only binders were removed by heat considering the solid loading because the solid loading of 59 vol% corresponds to 92.5 wt%. It is necessary to consider shape retention of component without the formation of defects because an inhomogeneous binder extraction generated by inappropriate debinding condition is sufficient to result in defects related to shape retention. A factor

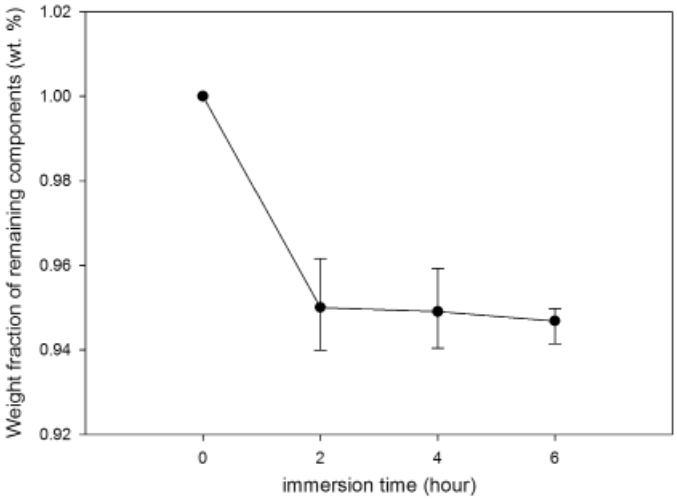

Fig. 4. Binder extraction for solvent debinding

affecting shape retention is heating rate. Uneven extraction of binder induced by dramatic variation in temperature, i.e., high heating rate, leads to distortion. To remove the binder without disruption of powder, the multiple-step of temperature condition was designed as illustrated in Fig. 5c

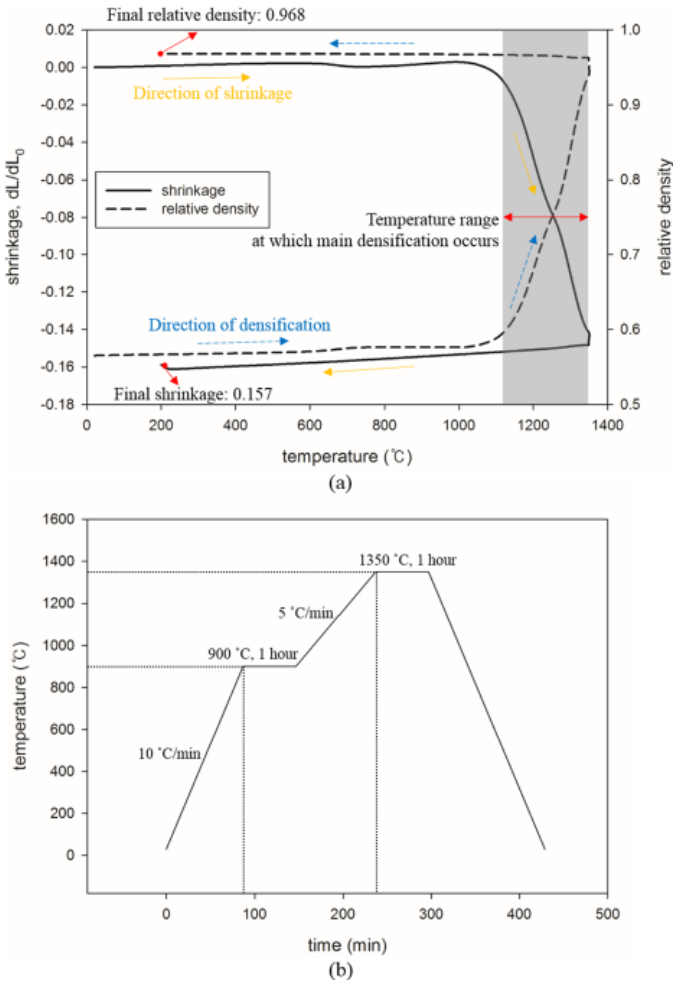

Fig. 6. Densification behavior during sintering; heating rate 10°C/min and H_2 atmosphere, and (b) optimized processing conditions for sintering

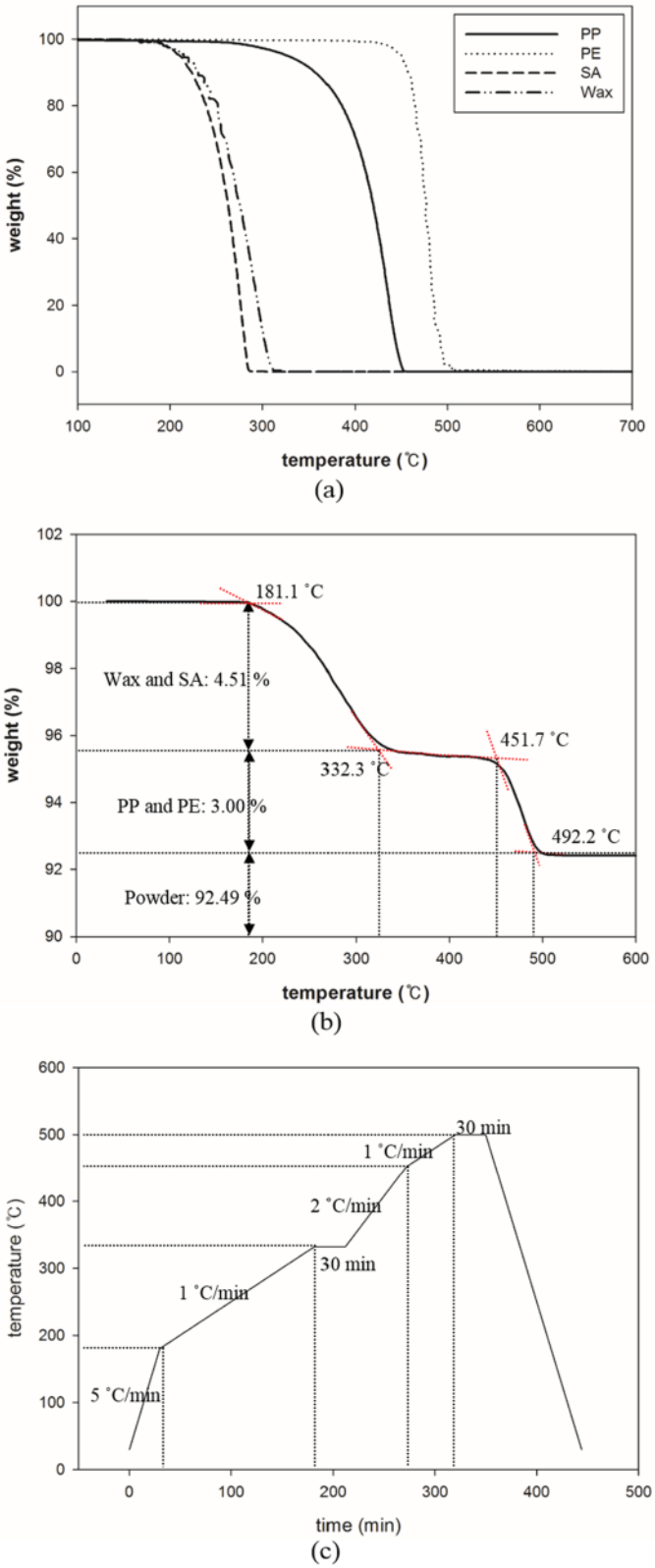

Fig. 5. TGA of binder system in H_2 atmosphere; (a) weight loss of binder system, (b) weight loss of feedstock, and (c) processing conditions for thermal debinding

The *in-situ* shrinkages measured by dilatometry experiments (DIL 402C, Netzsch) during sintering are presented in Fig. 6a. The final shrinkage, after sintering, was approximately 0.16% compared with the initial length. Shrinkage was considered to satisfy the dimensional tolerance of final components.

The relative density with respect to the mechanical strength was calculated by Eq. 1. The final relative density was 96.8% of the true density of powder. Based on the result of dilatometry experiment, the thermal cycle for sintering was determined. As illustrated in Fig. 6a, the main densification occurred in the temperature ranges from approximately 1100 to 1350°C. Distortion of a component is associated with the time-temperature combination. According to Wall et al. [26], high heating rate

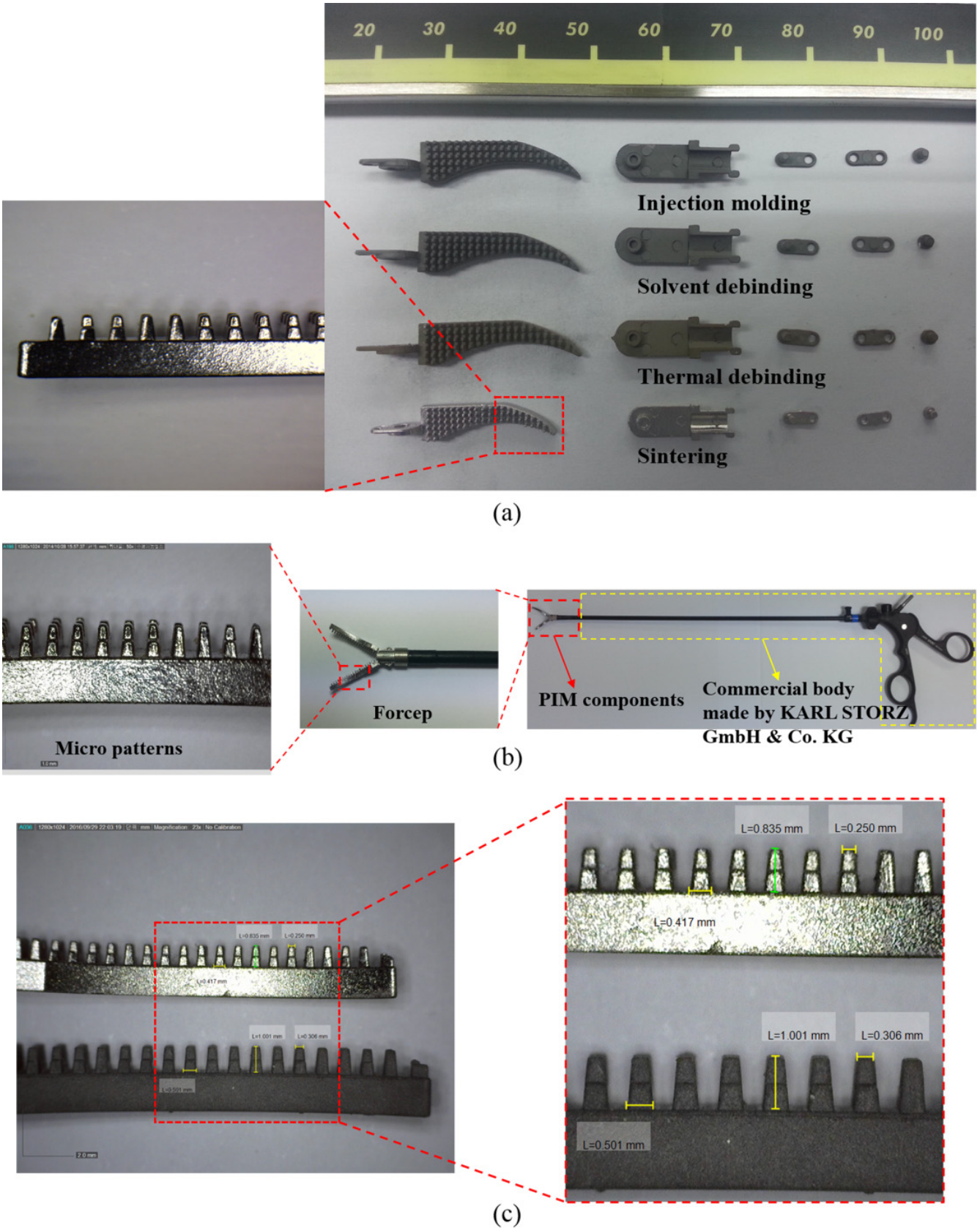

Fig. 7. (a) Injection molded, debound, and sintered components, (b) assembled components, (c) injection molded and sintered forceps

caused distortion. In this regard, the sinter cycle with respect to time-temperature was designed as illustrated in Fig. 6b. A relatively low heating rate of 5°C/min was employed in the main densification region. Finally, components for the surgical forceps were produced. Fig. 7 illustrates the injection molded, debound, and sintered components. The final relative density of sintered components measured by Archimedes' water immersion method was 97% of the theoretical value. This value was approximately identical to numerically estimated relative density. All components produced by PIM were assembled as illustrated in Fig. 7b.

To develop a hydrophobic surface on the micro pattern of surgical forceps, a target surface with rough microstructure and low surface energy, is essential. Despite the high mechanical and chemical resistance of stainless steel, a rough structure of the pattern with low surface energy was formatted by etching with a highly concentrated acid – 40 % ferric chloride solution – for 12 h. The hydrophobic surface, after chemical etching, was finally fabricated by the self-assembled monolayer method (SAM), i.e., the rough structure after being dried was dipped into Heptadecafluoro-1,1,2,2-tetrahydrodecyl trichlorosilane with *n*-hexane (volumetric ratio 1:1000) for 4 h to generate the hydrophobic surface. Fig. 8a,b illustrate the contact angle results of tested samples. The contact angles of the untreated and treated surfaces were 54.9° and 125.7°, respectively. Fig. 8c,d illustrate the hydrophobic component. This result indicated that a hydrophobic surface for surgical forceps was successfully fabricated using the treatment adopted in this study.

4. Conclusions

The hydrophobic surgical forceps were produced through PIM and surface treatment techniques. The processing conditions for PIM were established through several experiments and analysis. The solid loading for feedstock was determined to be 59 vol% to impart sufficiently low viscosity for molding and maintain the desired shape. The feedstock mixed by the twin-extruder mixer has homogenous distribution of powder in

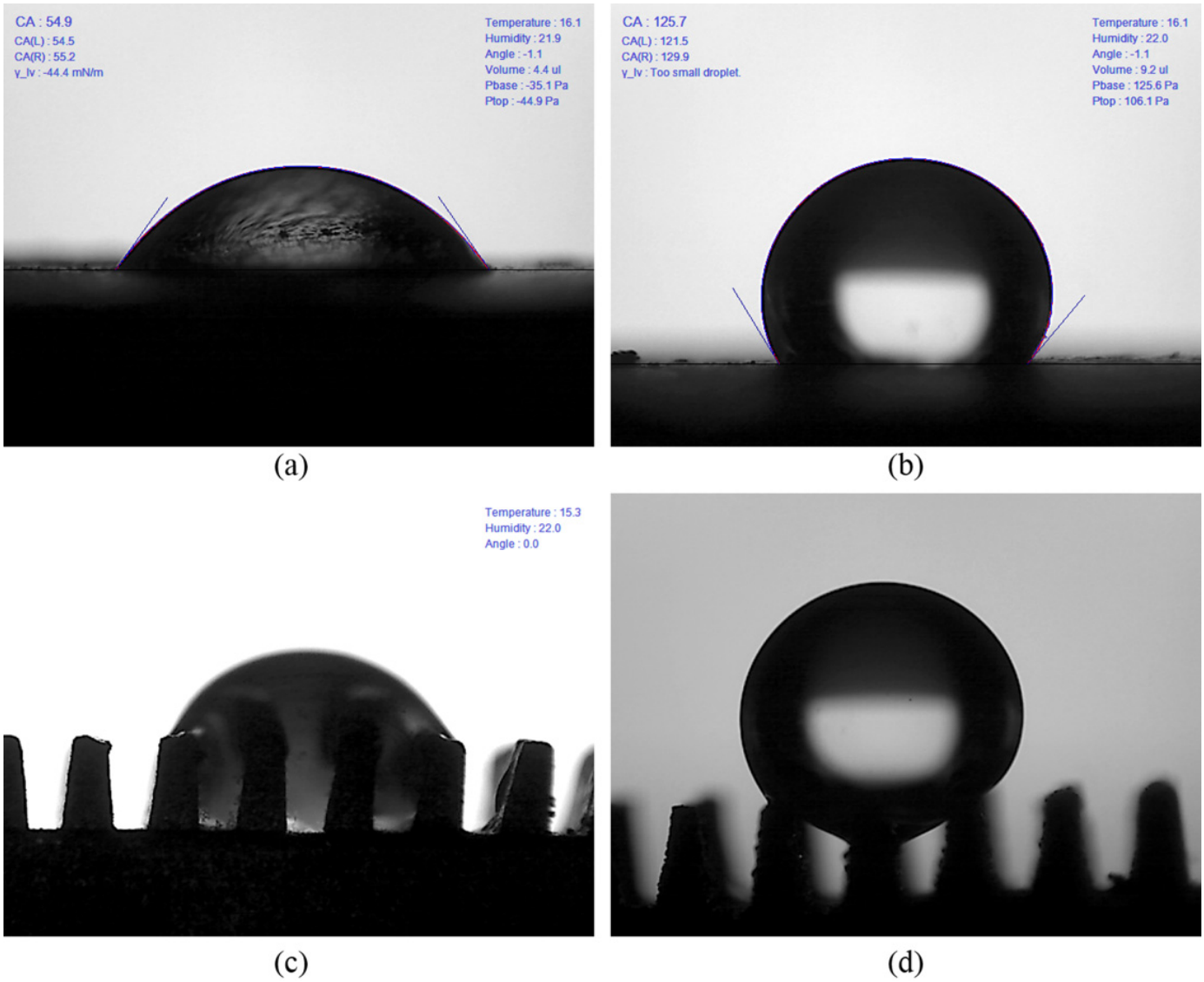

Fig. 8. Contact angle images (a) before surface treatment and (b) after surface treatments; hydrophobic surface of surgical forceps (c) before surface treatment and (d) after surface treatments

a specified binder system. The optimum debinding conditions with respect to immersion time and temperature were designed through the weight measurement method and TGA experiments to ensure shape retention without defects such as distortion or cracks. Based on the result of dilatometry experiment, the mold was appropriately designed considering the shrinkage during sintering. In addition, it is confirmed that the final sintered components attained near-full density. From the result, it can be estimated that the forceps produced by PIM have sufficient strength for application as surgical forceps. The hydrophobic surface on the surgical forceps was successfully created using surface treatment methods.

Acknowledgements

This research was supported by National Research Foundation of Korea (NRF) grant funded by the Korea government (MSIT) (No. 2011-0030075) and was conducted under the framework of Research and Development Program at the Korea Institute of Energy Research (KIER) (B8-2413-03).

REFERENCES

[1] L.P. Yeo, S.H. Ng, Z. Wang, Z. Wang, N.F. de Rooij, Microelectron. Eng. **86** (4), 933-936 (2009).

[2] R.M. German, A. Bose, Injection molding of metals and ceramics, 1997 Princeton, New Jersey.

[3] D. Heaney, Handbook of metal injection molding, 2012 Woodhead Publishing, Philadelphia.

[4] S. Ahn, S. Chung, S. Atre, S. Park, R. German, Powder Metall. **51** (4), 318-326 (2008).

[5] B. Huang, S. Liang, X. Qu, J. Mater. Process. Tech. **137** (1), 132-137 (2003).

[6] G. Aggarwal, S.J. Park, I. Smid, Int. J. Refrac. Met. H **24** (3), 253-262 (2006).

[7] A. Yakimov, T. Coyle, J. Mater. Sci. Lett. **19** (24), 2255-2257 (2000).

[8] W.J. Tseng, C.-K. Hsu, Ceram. Int. **25** (5), 461-466 (1999).

[9] K. Krishnamurthy, S.J. Lombardo, J. Ceram. Process. Res. **11** (4), 405-410 (2010).

[10] D.-M. Liu, W.J. Tseng, Ceram. Int. **24** (6), 471-481 (1998).

[11] J. Song, J. Evans, M. Edirisinghe, E. Twizell, J. Mater. Res. **15** (2), 449-457 (2000).

[12] R.K. Enneti, S.J. Park, R.M. German, S.V. Atre, Mater. Manuf. Process. **27** (2), 103-118 (2012).

[13] K. Hwang, T. Tsou, Metall. Mater. Trans. A **23** (10), 2775-2782 (1992).

[14] S.H. Chung, K.-S. Kwon, S.J. Park, R.M. German, Metals Process Simulation, ASM Handbook, 2010, ASM International, Materials Park, Ohio,

[15] J.-Y. Shiu, C.-W. Kuo, W.-T. Whang, P. Chen, Lab. Chip **10** (5), 556-558 (2010).

[16] T. Ishizaki, N. Saito, O. Takai, Langmuir **26** (11), 8147-8154 (2010).

[17] L. Hong, T. Pan, Microfluid Nanofluid **10** (5), 991-997 (2011).

[18] B. Bhushan, Y.C. Jung, Prog. Mater. Sci. **56** (1), 101-108 (2011).

[19] C.-C. Chang, F.-H. Huang, H.-H. Chang, T.-M. Don, C.-C. Chen, L.-P. Cheng, Langmuir **28** (49), 17193-17201 (2012).

[20] L. Cao, A.K. Jones, V.K. Sikka, J. Wu, D. Gao, Langmuir **25** (21), 12444-12448 (2009).

[21] Y. Chen, S. Chen, F. Yu, W. Sun, H. Zhu, Y. Yin, Surf. Interface Anal. **41** (11), 872-877 (2009).

[22] C.-H. Xue, S.-T. Jia, J. Zhang, J.-Z. Ma, Sci. Technol. Adv. Mater. **11** (3), 033002-1 (2010).

[23] P. Roach, N.J. Shirtcliffe, M.I. Newton, Soft Matter. **4** (2), 224-240 (2008).

[24] H.O. Gulsoy, C. Karatas, Mater Design **28** (9), 2488-2491 (2007).

[25] J.P. de Souza, S.V. Atre, P.K. Suri, J.A. Thomas, R.M. German, Congresso Anual Da ABM, Sao Paulo, 2003.

[26] P.A. Walls, J. Ferenczy, S. Moricca, P. Bendeich, T. Eddowes, An Investigation of Sintering Distortion in Full-Size Pyrochlore Rich Titanate Wasteform Pellets Due to Rapid Heating to 1350°C in Air, Environmental Issues and Waste Management Technologies in the Ceramic and Nuclear Industries VII, 2002, The American Ceramic Society, Westerville, Ohio.